PERGAMON

Carbon 40 (2002) 685–694

CARBON

A review of the effects of covapors on adsorption rate coefficients of organic vapors adsorbed onto activated carbon from flowing gases

G.O. Wood*

Los Alamos National Laboratory, Mail Stop K-486, Los Alamos, NM 87545, USA

Received 2 January 2001; accepted 3 June 2001

Abstract

Published breakthrough time, adsorption rate, and capacity data for components of organic vapor mixtures adsorbed from flows through fixed activated carbon beds have been analyzed. Capacities (as stoichiometric centers of constant pattern breakthrough curves) yielded stoichiometric times τ, which are useful for determining elution orders of mixture components. Where authors did not report calculated adsorption rate coefficients k_v of the Wheeler (or, more general, Reaction Kinetic) breakthrough curve equation, we calculated them from breakthrough times and τ. Ninety-five k_v (in mixture)/k_v (single vapor) ratios at similar vapor concentrations were calculated and averaged for elution order categories. For 43 first-eluting vapors the average ratio (1.07) was statistically no different (standard deviation 0.21) than unity, so that we recommend using the single-vapor k_v for such. Forty-seven second-eluting vapor ratios averaged 0.85 (standard deviation 0.24), also not significantly different from unity; however, other evidence and considerations lead us to recommend using k_v (in mixture) $= 0.85k_v$ (single vapor). Five third- and fourth-eluting vapors gave an average of 0.56 (standard deviation 0.16) for a recommended k_v (in mixture) $= 0.56k_v$ (single vapor) for such.

Keywords: A. Activated carbon; C. Adsorption; D. Adsorption properties

1. Introduction

Fixed beds of granular activated carbon are routinely used for removing toxic organic vapors from air flowing through them. Applications range from small sampling tubes to large air-cleaning facilities at nuclear power plants. An application of concern to industrial and government workers is respiratory protection using air-purifying respirators and associated organic vapor-removing cartridges.

Such beds and cartridges containing them will eventually get 'used up' after continuous exposure to vapors. The time at which an unwanted vapor penetrates the bed and reaches a defined, unacceptable concentration is called the breakthrough time of the vapor and the service life of the cartridge. Detecting or predicting breakthrough time(s) is essential for setting change-out schedules and maintaining worker protection.

Theories of adsorption of single vapors and associated equations for predicting breakthrough times are at advanced stages of development [1,2]. However, in actual applications there is often more than one organic vapor to be removed from air. Descriptive theories and predictive equations for multiple vapor removal are much less advanced. One multiple vapor effect is competition for adsorption volume. Another is displacement of one adsorbed vapor by another in the flowing air. Both are largely due to competitive equilibrium adsorption. Theories and data for multiple vapor equilibrium adsorption have been recently reviewed [3].

Adsorption rates, as well as adsorption capacities, must be considered in flowing air applications. Adsorption rate theories and correlations have also been reviewed for single vapors [2]. The most successful predictive equations for single organic vapors were found to be the empirical equations of Wood and Stampfer [4] and Lodewyckx and Vansant [5].

Less defined is the effect of a second or third organic vapor (covapor) on the adsorption rate of another. Limited

*Tel.: +1-505-667-9824; fax: +1-505-665-2192.
E-mail address: gerry@lanl.gov (G.O. Wood).

0008-6223/02/$ – see front matter
PII: S0008-6223(01)00185-3

rate results with large experimental uncertainties have led to conflicting conclusions. Therefore, the objective of the work reported here was to consolidate these results, reanalyze relevant published data, and attempt to come to conclusions based on larger data sets.

In this paper we are not considering water as a covapor, since it is a unique case in activated carbon beds. It differs significantly from organic vapors in adsorption isotherm shape, adsorption rate, and miscibility. Lodewyckx and Vansant [6] have reported and modeled effects of adsorbed water and water in the vapor phase on adsorption rate coefficients.

2. Background

2.1. Single vapors

Fig. 1 shows the characteristics of a carbon bed breakthrough curve (relative effluent concentration vs. time) for a single vapor at fixed airflow and challenge vapor concentration. It is a simple 'S-shaped' curve around a reference point called the stoichiometric center, which is determined by vapor concentration, flow rate, and adsorption capacity. Steepness and shape of the breakthrough curve is determined by the adsorption rate(s) involved. The breakthrough curve measured at the exit of the bed is the reflection of the corresponding vapor front profile moving through the bed.

The simplest, most often derived, and most widely used equation for describing a breakthrough curve is best called by its generic designation [7], the Reaction Kinetic Equation. In terms and units often associated with the Modified Wheeler Equation [8,9], the Reaction Kinetic Equation for breakthrough time t_b (min) is

$$t_b = \frac{W_e W}{C_o Q} - \frac{W_e \rho_B}{k_v C_o} \ln\left(\frac{C_o - C}{C}\right) \quad (1)$$

where C_o (g/cm^3) is the entering (challenge) concentration, C is the exit concentration, W_e is the gravimetric (g/g carbon) capacity, W is the weight (g) of carbon, Q (cm^3/min) is the volumetric air flow rate, ρ_B is the packed density (g/cm^3) of the carbon bed, and k_v (min^{-1}) is an overall adsorption rate coefficient. The first term of Eq. (1) is the stoichiometric center (time) of the breakthrough curve, which represents the breakthrough time at infinitely fast adsorption rate and large k_v.

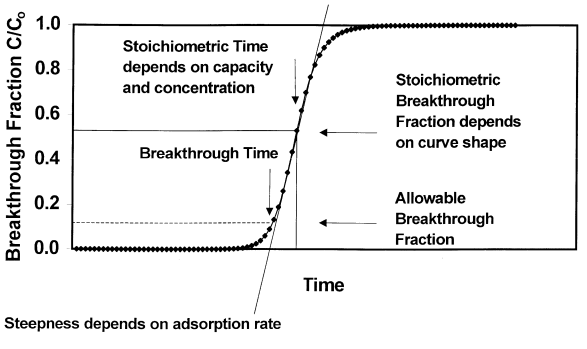

Fig. 1. Single vapor breakthrough curve characteristics.

The Modified Wheeler Equation [8]:

$$t_b = \frac{W_e W}{C_o Q} - \frac{W_e \rho_B}{k_v C_o} \ln\left(\frac{C_o}{C}\right) \quad (2)$$

substitutes $\ln(C_o/C)$ for $\ln[(C_o - C)/C]$, which makes less than 1% difference in the second (kinetic) term for breakthrough fractions C/C_o less than 0.032. However, it does change the shape of the breakthrough curve from 'S'-shaped to 'J'-shaped, approaching infinity instead of a maximum value ($C/C_o = 1$) at long times. Not realizing this and using the Modified Wheeler Equation at breakthrough fractions higher than 0.032 can lead to significant errors in analyzing data or calculating breakthrough times.

The Reaction Kinetic Equation is based on assuming a constant pattern (in-bed vapor profile or wavefront shape) and a constant overall rate coefficient [7]. This assumption allows Eq. (1) or (2) to be used variously to derive W_e and k_v from experimental data [9]:

(a) breakthrough time t_b vs. bed weight W at fixed breakthrough fraction C/C_o;
(b) t_b vs. bed residence time $W/Q\rho_B$ at fixed C/C_o;
(c) $\ln[(C_o - C)/C]$ or $\ln[C_o/C]$ vs. time t_b for varying C/C_o.

One difficulty in using approaches (a) and (b) is that k_v is obtained from the reciprocals of extrapolated intercepts, which, if close to zero, can introduce large uncertainties in the calculated values. The k_v from approach (c) is based on the slope of a plot of many points; however, it may represent only the value near the midpoint of the portion of the breakthrough curve included, not at other breakthrough fractions of concern.

In reality, non-ideal behavior is often observed. (a) The breakthrough curve may be steeper at small C/C_o than at corresponding $(1 - C/C_o)$, reflecting changing adsorption rate-limiting steps [10]. (b) Axial dispersion [11] may cause the profile to spread out more (apparent k_v to decrease) the longer the wavefront is in the bed. Yoon and Nelson [12] introduced an empirical time dependence for k_v to account for observed asymmetric breakthrough curves, particularly those associated with high humidities. Wood [13] developed a flexible empirical asymmetric breakthrough curve that reduces to the ideal, Eq. (1). Lavanchy and Stoeckli [14] used a linear reduction (0.01 at no adsorption to 1.0 at maximum bed loading) of the film diffusion coefficient (therefore of k_v) to account for

observed mass transfer rate decreases with increasing loading.

2.2. Multiple vapors

Typical breakthrough curves for components of a binary mixture of organic vapors in air are shown in Fig. 2. Compared with what would happen with a single vapor, breakthrough times are decreased, since each vapor wavefront moves through the bed faster as the other vapor is taking up some adsorption volume [i.e., effective W_e values are decreased in Eq. (1)]. Also, the less strongly, previously adsorbed vapor will be partially displaced by the other, resulting in a higher maximum concentration C_m of the former within sections of the bed than the C_o entering the bed ('rollup' or 'overshoot' phenomenon). Both breakthrough curves have stoichiometric centers that are determined by adsorption capacities in the mixed vapor situations at the effective values of C_o [3].

Steepness of the breakthrough curves, and therefore derived k_v, may be affected by the presence of another vapor. The vapor moving fastest through the bed and eluting first should encounter the same environment and be adsorbed at the same rate(s) as if it were a single vapor at the same effective challenge concentration $C_o = C_m$. However, if its breakthrough curve overlaps that of the next eluting one, there may be some interference with its adsorption rate [15].

The slower-eluting vapor, even if its breakthrough curve is well separated from the first, will encounter a different environment than if it were the only vapor. If its adsorption rate is determined only by external mass transfer (diffusion from air to the carbon surface), there may be no effect of the displacement and desorption of the covapor(s), especially at low concentrations [16]. If its adsorption rate is surface adsorption limited, the presence of another vapor occupying surface sites should slow down the adsorption rate, decreasing k_v. If it is pore diffusion limited, diffusion of the covapor could also reduce k_v [16].

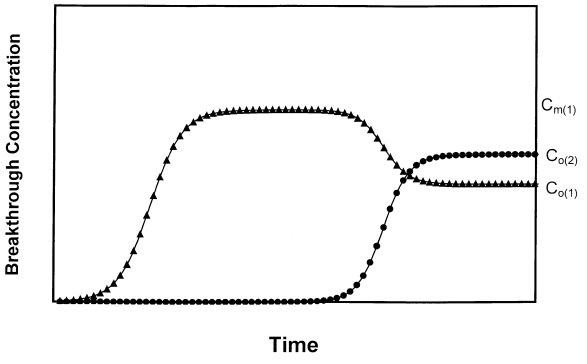

Fig. 2. Multiple vapor breakthrough curve characteristics. Circles represent the vapor (2) which has the higher adsorption capacity at its entering vapor concentration $C_{o(2)}$. Triangles represent the first-eluting vapor (1), whose maximum rollup concentration $C_{m(1)}$ exceeds its entering vapor concentration $C_{o(1)}$ due to displacement by Vapor 2.

3. Literature review of covapor effects on kinetics

Jonas and coworkers [17] studied breakthroughs of single vapors (carbon tetrachloride, benzene, and chloroform) and binary mixtures of them in dry nitrogen through samples of NACAR G-352 activated carbon (North American Carbon Company). They used small activated carbon beds (1–2.5 g, 1.06 cm diam.) of 6–10 mesh granules and small flows ($Q = 285$ cm^3/min) at 23°C. Plots of 1% breakthrough times vs. bed weights yielded adsorption capacities W_e (g/g) and rate coefficients k_v (min^{-1}) using Eq. (2). Table 1 lists reported k_v results for the vapor components in binary mixtures for which there was a corresponding determination for the same single vapor at a closely matching concentration (k_v also listed in Table 1). Ratios of the former to the latter are also listed. We converted experimental relative pressures to concentrations (ppm = moles of vapor per million moles of nitrogen mixture, including all vapors) using vapor pressures reported previously [18]; these concentrations appear in Table 1. We also calculated and list stoichiometric times [τ = first term in Eq. (1)] from W_e, C_o (g/cm^3 = ppm*M_w/RT in appropriate units), Q, and assuming a bed weight of $W = 1.0$ g. From these τ we can determine orders of elution (smaller τ means earlier eluting).

The vapor concentrations used by Jonas et al. [17] ranged up to 22 077 ppm, much higher than usually used in respirator cartridge or carbon studies (Table 1). The bed diameter (1.06 cm) was small compared with granule diameters (0.20–0.34 cm for 6–10 mesh). Relatively large granule sizes explain the relatively small values (Table 1) obtained for k_v [19]. The data analysis method ignores the rollup of the first-eluting vapor, defining k_v by assuming the Modified Wheeler Equation (2) single-vapor breakthrough curve between $t_{1\%}$ and τ and the maximum concentration as the entering C_o, not the rollup concentration. Ratios of k_v (in mixture)/k_v (single vapor) ranged from 0.96 to 1.28 (Table 1).

Swearengen and Weaver [20] challenged MSA respirator cartridges with isopropanol and methyl ethyl ketone, singly and in mixtures. The cartridges contained 12–20 mesh, petroleum-based activated carbon from WITCO Chemical Company. They used breakthrough times (averages of six measurements) at 1 and 10% C_o to calculate W_e and k_v (k_{ads} in their terminology) using the Modified Wheeler Equation (2). The k_v values and ratios for the two components for dry (20% relative humidity, RH) conditions only are listed in Table 1. We have calculated the stoichiometric times from W_e, assuming an apparent volumetric flow rate of 40 l/min [21] and carbon weight of 80.8 g for a pair of MSA cartridges [22]. Rollup was not

Table 1
Experimental rate coefficients and stoichiometric times for vapors singly and in mixtures[a]

Source	Elution order	Vapor	Conc. (ppm)	τ (min)	k_v (min^{-1})	k_v ratio	Covapor(s)	Conc. (ppm)	τ (min)	k_v (min^{-1})
Jonas [17]		Carbon tetrachloride	12 957	36	356					
	2	Carbon tetrachloride	13 082	25	454	1.28	Benzene	4049	19	557
		Chloroform	22 077	21	377					
	1	Chloroform	22 006	14	371	0.98	Benzene	10 823	15	500
		Benzene	10 675	44	411					
	2	Benzene	10 766	27	394	0.96	Chloroform	6958	15	470
	2	Benzene	10 915	22	473	1.15	Chloroform	10 968	17	446
	2	Benzene	10 823	15	500	1.22	Chloroform	22 006	14	371
Swearengen		Methyl ethyl ketone	2500	81	5300					
[20]	2	Methyl ethyl ketone	2500	37	4400	0.83	Isopropanol	5000	36	3700
		Isopropanol	4400	54	4200					
	1	Isopropanol	5000	36	3700	0.88	Methyl ethyl ketone	2500	37	4400
Swearengen		Methyl ethyl ketone	1000	144	5241					
[21]	1	Methyl ethyl ketone	1000	75	4804	0.92	Ethyl benzene	1000	155	3962
		Ethyl benzene	1000	192	4906					
	2	Ethyl benzene	1000	155	3962	0.81	Methyl ethyl ketone	1000	75	4804
	1	Methyl ethyl ketone	1000	60	6080	1.16	Hexanes	1000	82	2982
		Hexanes	1000	139	7100					
	2	Hexanes	1000	82	2982	0.42	Methyl ethyl ketone	1000	60	6080
		Butyl acetate	1000	167	7100					
	1	Butyl acetate	1000	75	3835	0.54	Ethyl benzene	1000	93	2955
	2	Ethyl benzene	1000	93	2955	0.60	Butyl acetate	1000	75	3835
		Isopropanol	1000	190	3456					
	1	Isopropanol	1000	86	4889	1.41	Methyl ethyl ketone	1000	97	4124
	2	Methyl ethyl ketone	1000	97	4124	0.79	Isopropanol	1000	86	4889
	2	Isopropanol	1000	84	3055	0.88	Ethyl benzene	1000	164	3345
	2	Ethyl benzene	1000	164	3345	0.68	Isopropanol	1000	84	3055
Cohen [22]		Carbon tetrachloride	1000	135	7548					
	1	Carbon tetrachloride	1000	97	12 911	1.71	Hexane	1000	114	16 089
	1	Carbon tetrachloride	1000	96	5260	0.70	Pyridine	1000	264	11 281
		Hexane	1000	123	24 303					
	2	Hexane	1000	114	16 089	0.66	Carbon tetrachloride	1000	97	12 911
		Pyridine	1000	270	14 033					
	2	Pyridine	1000	264	11 281	0.80	Carbon tetrachloride	1000	96	5260
Yoon [15]		Acetone	107	346	3070					
	1	Acetone	109	163	2812	0.92	*m*-Xylene	891	201	2989
		Acetone	260	245	2788					
	1	Acetone	248	154	3597	1.29	*m*-Xylene	730	254	5497
		Acetone	501	172	2801					
	1	Acetone	474	132	2764	0.99	*m*-Xylene	490	369	4950
		Acetone	726	139	3008					
	1	Acetone	749	122	2797	0.93	*m*-Xylene	260	682	5612
		Acetone	1060	110	2970					
	1	Acetone	813	117	2582	0.87	*m*-Xylene	90	1610	4485
		m-Xylene	93	1650	4208					
	2	*m*-Xylene	90	1610	4485	1.07	Acetone	813	117	2582
		m-Xylene	257	701	5227					
	2	*m*-Xylene	260	682	5612	1.07	Acetone	749	122	2797
		m-Xylene	446	386	5765					
	2	*m*-Xylene	490	369	4950	0.86	Acetone	474	132	2764
		m-Xylene	857	215	5068					
	2	*m*-Xylene	730	254	5497	1.08	Acetone	248	154	3597
		m-Xylene	973	206	5209					
	2	*m*-Xylene	891	201	2989	0.57	Acetone	109	163	2812

Table 1. Continued

Source	Elution order	Vapor	Conc. (ppm)	τ (min)	k_v (min^{-1})	k_v ratio	Covapor(s)	Conc. (ppm)	τ (min)	k_v (min^{-1})
Yoon [24]	1	Acetone	92	240	3178	1.04	Styrene	508	373	5043
	1	Acetone	99	239	2996	0.98	Styrene	516	380	4650
	1	Acetone	305	169	3140	1.13	Styrene	503	386	6030
	1	Acetone	479	137	2625	0.94	Styrene	507	367	4703
	1	Acetone	779	115	2957	0.98	Styrene	510	385	4785
	1	Acetone	985	102	2710	0.91	Styrene	496	405	4339
	1	Acetone	464	146	3473	1.24	Styrene	228	726	5912
	1	Acetone	492	124	2439	0.87	Styrene	733	270	5635
	1	Acetone	494	113	3293	1.18	Styrene	1036	206	4503
	1	Acetone	490	93	3149	1.12	Styrene	1578	134	3733
	1	Acetone	97	158	3098	1.01	Styrene	892	217	4436
	1	Acetone	234	129	2847	1.02	Styrene	739	257	4059
	1	Acetone	249	136	3351	1.20	Styrene	755	267	5687
	1	Acetone	746	126	2808	0.93	Styrene	256	762	4670
		Styrene	481	419	7165					
		Styrene	497	392	5653					
	2	Styrene	508	373	5043	0.79	Acetone	92	240	3178
	2	Styrene	516	380	4650	0.73	Acetone	99	239	2996
	2	Styrene	503	386	6030	0.94	Acetone	305	169	3140
	2	Styrene	507	367	4703	0.73	Acetone	479	137	2625
	2	Styrene	510	385	4785	0.75	Acetone	779	115	2957
	2	Styrene	496	405	4339	0.68	Acetone	985	102	2710
		Styrene	254	728	6942					
	2	Styrene	228	726	5912	0.85	Acetone	464	146	3473
	2	Styrene	256	762	4670	0.67	Acetone	746	126	2808
		Styrene	725	270	6827					
	2	Styrene	733	270	5635	0.83	Acetone	492	124	2439
	2	Styrene	739	257	4059	0.59	Acetone	234	129	2847
	2	Styrene	755	267	5687	0.83	Acetone	249	136	3351
		Styrene	1045	206	6092					
	2	Styrene	1036	206	4503	0.74	Acetone	494	113	3293
	2	Styrene	1578	134	3733	0.61	Acetone	490	93	3149
	2	Styrene	892	217	4436	0.73	Acetone	97	158	3098
Lara [25]		Toluene	244	522	9698					
	1	Toluene	95	108	10 030	1.03	*m*-Xylene	875	131	4773
	1	Toluene	94	197	9245	0.95	*m*-Xylene	507	232	6011
	1	Toluene	245	136	11 202	1.16	*m*-Xylene	725	180	3986
	1	Toluene	242	135	11 032	1.14	*m*-Xylene	740	175	4779
	1	Toluene	249	167	9270	0.96	*m*-Xylene	510	232	4310
		Toluene	513	273	5669					
	1	Toluene	516	136	8624	1.52	*m*-Xylene	507	221	4177
		Toluene	746	204	8472					
	1	Toluene	747	146	11 231	1.33	*m*-Xylene	247	390	3180
	1	Toluene	757	109	7099	0.84	*m*-Xylene	505	194	3619
		Toluene	773	206	5390					
	1	Toluene	886	144	6550	1.22	*m*-Xylene	97	582	2579
		Toluene	1138	147	8651					
	1	Toluene	1026	90	10 188	1.18	*m*-Xylene	524	188	3082
		m-Xylene	247	557	8200					
	2	*m*-Xylene	97	582	2579	0.31	Toluene	886	144	6550
	2	*m*-Xylene	247	390	3180	0.39	Toluene	747	146	11 231
		m-Xylene	571	241	4865					
	2	*m*-Xylene	510	232	4310	0.89	Toluene	249	167	9270
	2	*m*-Xylene	507	221	4177	0.86	Toluene	516	136	8624
	2	*m*-Xylene	507	232	6011	1.24	Toluene	94	197	9245

Table 1. Continued

Source	Elution order	Vapor	Conc. (ppm)	τ (min)	k_v (min^{-1})	k_v ratio	Covapor(s)	Conc. (ppm)	τ (min)	k_v (min^{-1})
	2	*m*-Xylene	505	194	3619	0.74	Toluene	757	109	7099
	2	*m*-Xylene	524	188	3082	0.63	Toluene	1026	90	10 188
		m-Xylene	747	189	8341					
	2	*m*-Xylene	725	180	3986	0.48	Toluene	245	136	11 202
	2	*m*-Xylene	740	175	4779	0.57	Toluene	242	135	11 032
		m-Xylene	1093	118	8333					
	2	*m*-Xylene	875	131	4773	0.57	Toluene	95	108	10 030
Yoon [26]		Toluene	513	273	4182					
	3	Toluene	540	346	3055	0.73	Acetone (1150 ppm) and cyclohexane (1030 ppm)			
	2	Toluene	500	277	2926	0.70	*m*-Xylene (300 ppm) and cyclohexane (500 ppm)			
	3	Toluene	500	331	2986	0.71	Ethyl acetate (970 ppm) and cyclohexane (1210 ppm)			
		Acetone	1060	110	2970					
	1	Acetone	1150	73	3001	1.01	Toluene (540 ppm) and cyclohexane (1030 ppm)			
	1	Acetone	1160	66	3380	1.14	Cyclohexane (1010 ppm), toluene (490 ppm), *m*-xylene (300 ppm)			
		m-Xylene	247	557	6050					
	3	*m*-Xylene	300	581	2415	0.40	Toluene (500 ppm) and cyclohexane (500 ppm)			
	4	*m*-Xylene	300	554	2671	0.44	Acetone (1160 ppm), cyclohexane (1010 ppm), toluene (490 ppm)			
	4	*m*-Xylene	280	597	3019	0.50	Ethyl acetate (740 ppm), cyclohexane (510 ppm), toluene (510 ppm)			
Robbins [27]		*p*-Xylene	3662	77	4158					
	2	*p*-Xylene	3418	57	2862	0.69	Toluene	3418	16	
		p-Xylene	2197	128	4080					
	2	*p*-Xylene	2686	58	3114	0.76	*p*-Fluorotoluene	2442	27	
		p-Xylene	1221	226	3744					
	1	*p*-Xylene	977	158	4686	1.25	*p*-Dichlorobenzene	977	904	
	1	*p*-Xylene	977	124	4692	1.25	*o*-Dichlorobenzene	1221	1435	
		Pyrrole	2662	96	4056					
	2	Pyrrole	3662	52	4788	1.18	Toluene	3662	15	
		Pyrrole	2930	127	3900					
	2	Pyrrole	2930	65	4098	1.05	*p*-Fluorotoluene	2930	33	
		Pyrrole	977	403	3636					
	1	Pyrrole	977	153	4062	1.12	*p*-Dichlorobenzene	977	753	
	1	Pyrrole	977	174	4386	1.21	*o*-Dichlorobenzene	977	1307	

[a] Carbons are identified and described in the text.

considered; the two compounds eluted closely together ($\tau = 36$ and 37 min) at the concentrations used. Ratios of k_v (in mixture)/k_v (single vapor) were 0.83 and 0.88.

These authors did additional work with these compounds and the same MSA cartridges and reported 1 and 10% breakthrough times [21]. We have used these times and the Reaction Kinetic Equation (1) to calculate (iteratively) the stoichiometric times, rate coefficients, and ratios listed in Table 1 for the dry (50% RH) conditions. Again, we used the Cohen et al. [22] MSA cartridge carbon weight and packing density (0.43 g/cm^3). Ratios of k_v (in mixture)/k_v (single vapor) ranged from 0.42 to 1.41.

Zwiebel and coworkers [10,23] studied mixtures of benzene and dichloromethane on three carbons at three to five concentrations. Small beds (<2 g, 1.25 cm diam.) of 12–30 mesh BPL activated carbon, ASC impregnated BPL carbon, and TEDA impregnated carbon were used. Mass transfer coefficients extracted from plots of $t_{1\%}/W$ vs.

W_e/C_o at constant $Q = 2$ l/min for both single vapors and components of binary mixtures were presented in graphs, but not tabulated numerically; therefore, they do not appear in Table 1. They concluded that for dichloromethane, the first-eluting vapor, the rate coefficients were ''essentially identical'' in the mixtures as in the single component experiments. Actually, for all three carbons the k_v (in mixture) were ''somewhat larger'' than the k_v (single vapor), which they attributed to the rollup (overshoot) effect not being considered in the calculations. In the case of benzene, the second-eluting vapor, the mass transfer coefficients were ''substantially lower'' than the corresponding single-component ones. The authors explained this as likely due to ''counter diffusion of molecules, as manifest by the simultaneous adsorption of C_6H_6 and desorption of CH_2Cl_2,....'' Vapor concentration effects on mass transfer coefficients and ratios were mixed, so that no conclusions could be reached about this.

Cohen and coworkers [22] studied carbon tetrachloride, hexane, and pyridine vapors singly and in binary mixtures in air passed through MSA cartridges and respirator carbon tubes. They plotted 10% breakthrough times vs. residence times [method (b) above] for different flow rates Q and carbon weights W to extract W_e and k_v from the slopes and intercepts using the Modified Wheeler Equation (2). Table 1 lists reported k_v, as well as k_v (in mixture)/k_v (single vapor) ratios (0.66–1.71) and stoichiometric times that we have calculated from the reported capacities W_e, C_o, Q = 28.4 l/min, and $W = 40.5$ g. Cohen et al. concluded that: ''None of the k_v values for mixtures of adsorbates showed statistically significant differences from those obtained with individual components.'' and ''The large standard deviations [21–103%] in the estimates of k_v reflect the sensitivity of this parameter to changes in the y-axis intercept that have been previously observed.''

Yoon and coworkers studied single vapors and binary mixtures of acetone/m-xylene [15] and acetone/styrene [24]. They used Scott Aviation Model 642-OV respirator cartridges containing 50 g (112 cm^3) of 12–20 mesh, coconut-based activated carbon at an air flow rate of 24 l/min. Breakthrough curve data were fit as $\ln[P/(1-P)]$ vs. time t to the following linear form of the Reaction Kinetic Equation:

$$t = \tau + \frac{1}{k'} \ln\left(\frac{P}{1-P}\right) \tag{3}$$

where in terms used in Eq. (1), $P = C/C_o$ or C/C_m, $\tau = W_e W/C_o Q$, and $k' = k_v C_o/W_e \rho_B$. Rollup ($C_m > C_o$ for the first-eluting vapor) was recognized, so that τ is the true breakthrough curve midpoint and k' is at that midpoint. They found that the unitless product $k = k'\tau$ was apparently invariant with concentration for single vapors: acetone (13.9±0.4 standard deviation for 107–1060 ppm), m-xylene (23.7±2.7 for 93–973 ppm), and styrene (30.3±3.1 for 254–1045 ppm). This conclusion is equivalent to saying k_v is invariant with concentration, as has been reported elsewhere [4]. They also concluded [15] that ''the value of each k' for single-component m-xylene [the later eluting vapor vs. acetone] is similar to that of the corresponding [similar concentration] k' of the binary system except for the special case [of overlapping breakthrough curves]. In this [overlapping] case, the binary k' is less [0.0694 min^{-1}] than the single component k' [0.112 min^{-1} interpolated].'' We have confirmed this by calculating and averaging $k'\tau$ for acetone (13.6±1.8 including the overlapping case) and m-xylene (24.0±2.4 excluding the overlapping case). Similarly, in acetone/styrene mixtures [24] the averages were 14.0±1.4 for acetone and 22.7±3.3 for styrene, the later-eluting vapor. We have calculated $k_v = k'\tau Q\rho_B/W$ from reported k' and τ values and listed them and their ratios in Table 1.

Lara and coworkers [25] continued this approach with toluene/m-xylene mixtures at 36 l/min, 25°C, and the same cartridges as Yoon et al. [15,24]. However, they reported the results as total volumetric capacity W_v (cm^3/cartridge) $= W_e W/d_L$, where d_L is the normal liquid density, or as stoichiometric time τ (in single vapor cases) and as 10% breakthrough time $t_{10\%}$. For Table 1 we calculated $\tau = 10^6 W_v RT/QC_o V_m$, using molar volumes V_m (cm^3/mol) and C_o (ppm) given in this reference [25]. We also calculated rate coefficients from the Reaction Kinetic Equation (1) as $k_v = [10^3 \tau Q \rho_B \ln(9)]/[W(\tau - t_{10\%})]$ and included them and their ratios in Table 1.

In one more study Yoon and coworkers [26] measured and analyzed breakthrough curves for components of ternary (acetone/cyclohexane/toluene, m-xylene/cyclohexane/toluene, ethyl acetate/cyclohexane/toluene) and quaternary (acetone/cyclohexane/toluene/m-xylene, ethyl acetate/cyclohexane/toluene/m-xylene) vapor mixtures. Flow rate was 24 l/min for the same Scott Aviation cartridges [15,24]. They reported results as k' and τ, from which we have calculated k_v, as described above. Unfortunately, they did not report single-vapor results at corresponding concentrations and flow rates. Therefore, we took as corresponding single-vapor rate coefficients for Table 1 a 1060 ppm acetone k_v calculated from Ref. [15] along with 513 ppm toluene and 247 ppm m-xylene k_v from Ref. [25]. The latter two k_v had to be corrected from 36 to 24 l/min using ratios of flow rates to the 0.75 power [5].

Robbins and Breysse [27,28] studied the effects of four probe covapors (toluene, p-fluorotoluene, o-dichlorobenzene, p-dichlorobenzene) on the breakthrough curves (C/C_o from 0.0025 to 0.25) of p-xylene or pyrrole. Breakthrough curves of the covapors (probe vapors) were not measured; only their concentrations were reported. They used small samples (1.000 g, 0.6 cm diam.) of 12–20 mesh activated carbon from an American Optical R51A organic vapor respirator cartridge and small airflows (335–350 cm^3/min) at 24.4°C. They used the Modified Wheeler Equation (2) to obtain W_e (g/g) and k_v (s^{-1}) for con-

centrations C_o (μmol/cm^3) of toluene or pyrrole alone or in binary mixtures with probe vapors. For Table 1 we calculated τ from W_e for 342 cm^3/min average airflow.

Robbins and Breysse [27] concluded that: "... the k_v of *p*-xylene changes when *p*-xylene is in the presence of another vapor. The changes in k_v appear to depend on the relative difference between the boiling point of *p*-xylene and the accompanying probe vapor (i.e., k_v decreases with lower boiling point probe; k_v increases with higher boiling point probe)... . The k_v for pyrrole was always increased in the presence of a second vapor compared to the k_v of pyrrole alone." This suggests that the order of elution is important; therefore, we have estimated stoichiometric times for the probe vapors. First, we estimated probe vapor capacities from corresponding *p*-xylene or pyrrole capacities in mixtures using the Ideal Adsorbed Solution Theory solution of the Dubinin/Radushkevich isotherm equation [29] to get relative mole fractions at equilibrium. For this we took micropore volume $W_o = 0.5$ cm^3/g, relative (to benzene) adsorption potential $E_o = 10.95$ kJ/mol, affinity coefficients β (1.34 for *p*-xylene, 0.83 for pyrrole, 1.17 for toluene, 1.21 for *p*-fluorotoluene, and 1.32 for both *o*- and *p*-dichlorobenzene), and the vapor pressures at 24.4°C tabulated in Ref. [27]. We then calculated stoichiometric times τ listed in Table 1 for the probe covapors. The k_v (in mixture)/k_v (single vapor) ratios are 0.69 and 0.76 in the two cases in which *p*-xylene eluted later and greater than unity (1.05–1.25) in all the other cases, for which *p*-xylene or pyrrole eluted first. Note: the data collection and analysis method did not measure or account for rollups of the earlier-eluting compounds.

4. Results of new analyses

Table 1 lists elution orders of components of mixtures (1 = first eluting, 2 = second, etc.) obtained by comparing stoichiometric times τ. Ninety-five rate coefficient ratios k_v (in mixture)/k_v (single vapor) are listed from k_v reported or calculated at similar vapor concentrations and flow rates, as described above.

Since the above review of theory and data suggested that these ratios might be different depending on the order of elution in mixtures, the ratios have been averaged by elution-order categories. For 43 first-eluting mixture components the average k_v (in mixture)/k_v (single vapor) was 1.07 with a standard deviation of 0.21; for 47 second-eluting components it was 0.85 with a standard deviation of 0.24; for five third- or fourth-eluting components it was 0.56 with a standard deviation of 0.16.

5. Discussion and recommendations

The large standard deviations for these ratios are not surprising, considering the difficulties of extracting rate coefficients from breakthrough time or breakthrough curve data. Rate coefficient values depend on assumed breakthrough curve functions, reciprocals of extrapolations of breakthrough time data to graphical intercepts (sometimes near zero), or small differences in breakthrough times at differing breakthrough fractions. Breakthrough fraction values or ranges selected often differ among researchers.

The average k_v (in mixture)/k_v (single vapor) ratio (1.07) for first-eluting components is well within one standard deviation (0.21) of 1.00; therefore, we must say that this data set does not indicate any statistical difference between k_v for first-eluting components in mixtures and in single-vapor adsorption on carbon beds. There is also no theoretical reason why k_v should be different. The first-eluting vapor is adsorbed on activated carbon in its original condition, not changed by a later-eluting vapor. However, as we have discussed previously, the later-eluting vapor produces rollup by displacement, so that the rollup concentration of the earlier-eluting vapor, not the entering concentration, must be considered in applying k_v to estimate a breakthrough time. Therefore, with this caveat we recommend using the measured or estimated single vapor k_v for the first-eluting vapor of a mixture.

For second-eluting components the ratio of 0.85 is also within one standard deviation (0.24) of 1.00. However, in this case there are good reasons to expect k_v (in mixture)/k_v (single vapor) to be less than 1.00. As we have discussed previously, the second-eluting vapor in mixtures displaces some of the first, causing a mass transfer of the latter in a direction opposing the mass transfer of the former. It is easy to imagine that this would reduce the adsorption rate of the second (or any subsequent)-eluting vapor. Since the second-eluting vapor likely has a higher adsorption energy than the first, small heating effects may also occur. Also, axial dispersion, however significant, could be increased by these other effects, producing a smaller apparent k_v. Considering all these effects and the advantages of being conservative in worker protection or process design, we recommend using the factor 0.85 for second-eluting vapors, such that k_v (in mixture) = 0.85k_v (single vapor).

There were fewer data for calculating k_v (in mixture)/k_v (single vapor) ratios for third- and fourth-eluting vapors; therefore, we combined them for (somewhat questionable for $n = 5$) statistical analysis. Also, we had to use reference single-vapor k_v from related work (see above), sometimes with assumed flow rate corrections. Nevertheless, the average k_v (in mixture)/k_v (single vapor) = 0.56 ratio with 0.16 standard deviation seems to be significantly less than unity and less than for the second-eluting vapors. This is also reasonable, since two or more previously adsorbed components are being displaced, which should reduce k_v of the later-eluting vapor(s) even more than in the binary case. For the same reasons as in the preceding paragraph, therefore, we recommend using the factor of 0.56 for third- and subsequent-eluting vapors, such that k_v (in mixture) = 0.56k_v (single vapor).

These quantitative conclusions on the effects of order of

elution on k_v are in qualitative agreement with the conclusions of Zwiebel and coworkers [10], Yoon and coworkers [15,24], and Robbins and Breysse [27]. The Yoon [15] 'exception' (k_v ratio = 0.57 for second-eluting 891 ppm *m*-xylene and k_v ratio = 0.92 for first-eluting 109 ppm acetone) is also in qualitative agreement with our conclusions. Additional effects due to overlapping breakthrough curves are not clearly seen in our results. In the mixtures in Table 1 for which stoichiometric times of components differ by less than 20 min, five k_v ratios for first-eluting vapors average 1.10 (range 0.54–1.71) and eight k_v ratios for second-eluting vapors average 0.94 (range 0.60–1.28). However, conclusions from studies of bulk (non-flow) simultaneous adsorption of mixture components are that "...the component whose relative sorption uptake proceeds faster retards the internal mass transfer of the component having the lower value γ [relative sorption uptake]" [16]. Therefore, in cases of coincident or nearly coincident breakthrough curves, the lower k_v correction factor should be applied to both components (e.g., 0.85 instead of 1.0 for coincidently eluting binary components).

Uncertainties in rate coefficients and their ratios (for the reasons presented above) overwhelm effects of carbon differences, if any. They also make it difficult to prove or quantify the mechanisms and parameters that may alter adsorption rates. Fortunately, the contribution of kinetics [second term of Eq. (1)] to activated carbon bed breakthrough time is often minor compared with the contribution of capacity (first term), so that adsorption rate uncertainties contribute less to overall breakthrough time uncertainties.

References

[1] Wood GO. Estimating service lives of organic vapor cartridges. Am Ind Hyg Assoc J 1994;55:11–5.

[2] Wood GO. Reviews of models for adsorption of single vapors, mixtures of vapors, and vapors at high humidities on activated carbon for applications including predicting service lives of organic vapor respirator cartridges. Report LA-UR-00-1531. Los Alamos, NM: Los Alamos National Laboratory, 2000.

[3] Wood GO. Review and comparisons of D/R models of equilibrium adsorption of binary mixtures of organic vapors on activated carbons. Report LA-UR-00-5268. Los Alamos, NM: Los Alamos National Laboratory, 2000. Carbon 2001;40(3):231–9.

[4] Wood GO, Stampfer JF. Adsorption rate coefficients for gases and vapors on activated carbons. Carbon 1993;31:195–200.

[5] Lodewyckx P, Vansant EF. Estimating the overall mass transfer coefficient k_v of the Wheeler–Jonas equation: a new and simple model. Am Ind Hyg Assoc J 2000;61:501–5.

[6] Lodewyckx P, Vansant EF. The influence of humidity on the overall mass transfer coefficient of the Wheeler–Jonas equation. Am Ind Hyg Assoc J 2000;61:461–8.

[7] Vermeulen T, LeVan MD, Hiester NK, Klein G. Adsorption and ion exchange. In: Perry RH et al., editor, Perry's chemical engineers handbook, 6th ed., New York: McGraw-Hill, 1984, pp. 1–48, section 16.

[8] Jonas LA, Rehrmann JA. The kinetics of adsorption of organo-phosphorus vapors from air mixtures by activated carbons. Carbon 1972;10:657–63.

[9] Wood GO, Moyer ES. A review of the Wheeler equation and comparison of its applications to organic vapor respirator cartridge breakthrough data. Am Ind Hyg Assoc J 1989;50:400–7.

[10] Zwiebel I, Myers FR, Neusch DA. Multicomponent mass transfer in fixed-bed carbon adsorption columns. Carbon 1987;25:85–95.

[11] Copola AP, LeVan MD. Adsorption with axial diffusion in deep beds. Chem Eng Sci 1981;36:967–71.

[12] Yoon YH, Nelson JH. A theoretical study of the effect of humidity on respirator cartridge service life. Am Ind Hyg Assoc J 1988;49:325–32.

[13] Wood GO. Organic vapor respirator cartridge breakthrough curve analysis. J Int Soc Resp Prot 1993;10(4):5–17.

[14] Lavanchy A, Stoeckli F. Dynamic adsorption of vapour mixtures in active carbon beds described by the Myers–Prausnitz and Dubinin theories. Carbon 1997;35:1573–9.

[15] Yoon YH, Nelson JH, Lara J, Kamel C, Fregeau D. A theoretical interpretation of the service life of respirator cartridges for the binary acetone/*m*-xylene system. Am Ind Hyg Assoc J 1991;52:65–74.

[16] Marutovsky RM, Bulow M. Sorption kinetics of multicomponent gaseous and liquid mixtures on porous sorbents. Gas Sep Purif 1987;1:66–76.

[17] Jonas LA, Sansone EB, Farris TS. Prediction of activated carbon performance for binary vapor mixtures. Am Ind Hyg Assoc J 1983;44:716–9.

[18] Jonas LA, Tewari YB, Sansone EB. Prediction of adsorption rate constants of activated carbon for various vapors. Carbon 1979;17:345–9.

[19] Rehrmann JA, Jonas LA. Dependence of gas adsorption rates on carbon granule size and linear flow velocity. Carbon 1978;16:47–51.

[20] Swearengen PM, Weaver SC. The effect of organic-vapor mixtures on the service life of respirator cartridges. In: Proceedings of the 1985 Scientific Conference on Chemical Defense Research, MD: Chemical Research and Development Center, Aberdeen Proving Ground, 1986 (Report CRDC-SP-86007).

[21] Swearengen PM, Weaver SC. Respirator cartridge study using organic-vapor mixtures. Am Ind Hyg Assoc J 1988;49:70–4.

[22] Cohen HJ, Briggs DE, Garrison RP. Development of a field method for evaluating the service lives of organic vapor cartridges — Part III: Results of laboratory testing using binary organic vapor mixtures. Am Ind Hyg Assoc J 1991;52:34–43.

[23] Zwiebel I. Mixed gas adsorption on charcoal filters. Unpublished report. Tempe, AZ: Arizona State University, 1986.

[24] Yoon YH, Nelson JH, Lara J, Kamel C, Fregeau D. A theoretical model for respirator cartridge service life for binary systems: application to acetone/styrene mixtures. Am Ind Hyg Assoc J 1992;53:493–502.

[25] Lara J, Yoon YH, Nelson JH. The service life of respirator cartridges with binary mixtures of organic vapors. J Int Soc Resp Prot 1995;Spring:7–26.

[26] Yoon YH, Nelson JH, Lara J. Respirator cartridge service-

life: exposure to mixtures. Am Ind Hyg Assoc J 1996;57:809–19.
[27] Robbins CA, Breysse PN. The effect of vapor polarity and boiling point on breakthrough for binary mixtures on respirator carbon. Am Ind Hyg Assoc J 1996;57:717–23.
[28] Robbins CA. The effect of component polarity on the adsorption of binary organic vapor mixtures onto respirator carbon. Ph.D. thesis. Baltimore, MD: Johns Hopkins University, 1995.
[29] Lavanchy A, Stockli M, Wirz C, Stoeckli F. Binary adsorption of vapors in active carbons described by the Dubinin equation. Adsorp Sci Technol 1996;13:537–45.